A Quantitative Study of Electroporation Showing a Plateau in Net Molecular Transport

Mark R. Prausnitz,* Becky S. Lau,*‡ Christina D. Milano,*‡ Stewart Conner,§ Robert Langer,*‡ and James C. Weaver‡

*Department of Chemical Engineering, ‡Harvard/MIT Division of Health Sciences and Technology, and §Center for Cancer Research, Massachusetts Institute of Technology, Cambridge, Massachusetts 02139 USA

ABSTRACT Electroporation is believed to involve a temporary structural rearrangement of lipid bilayer membranes, which results in ion and molecular transport across the membrane. The results of a quantitative study of molecular transport due to electroporation caused by a single exponential pulse are presented; transport of four molecules of different physical characteristics across erythrocyte ghost membranes is examined as a function of applied field strength. Flow cytometry is used to quantitatively measure the number of molecules transported for 10^4 to 10^5 individual ghosts for each condition.

This study has four major findings: 1) Net transport first increases with field strength, but reaches a plateau at higher field strengths. Significant transport is found at or below 1 kV/cm, and transport plateaus begin at field strengths between 2 and 5 kV/cm depending on the molecule transported. 2) A single population of ghosts generally exists, but exhibits a wide distribution in the amount of molecular transport. 3) Under the conditions used, the direction of transport across the ghost membrane does not appear to affect molecular transport significantly. 4) Large numbers of ghosts may be destroyed by the electroporation procedure.

INTRODUCTION

Electroporation has rapidly progressed from an intriguing biophysical phenomenon to a method with wide-spread use in DNA transfection and other biological protocols (Neumann et al., 1989; Chang et al., 1992). Although the structure of the "pores" created by electroporation is not actually known, it is generally believed that they are transient aqueous pathways that perforate the membrane. While most pores are believed to close rapidly, some may remain open orders of magnitude longer than the duration of the pulse. Diffusion and movement directly due to the electric field (e.g., electrical drift and electro-osmosis) are likely mechanisms of molecular transport across cell membranes due to electroporation. While the mechanism of electroporation is not completely understood, numerous experiments show that electroporation occurs for short pulses when the transmembrane voltage reaches approximately 1 V. Characteristic electric field pulses causing electroporation of cells are 1–20 kV/cm (depending on cell size and orientation) and have durations of 10 μs to 10 ms.

Relatively few studies have made quantitative measurements of molecular transport (Mir et al., 1988; Chakrabarti et al., 1989; Lambert et al., 1990), particularly on a "transport per cell" basis (Bartoletti et al., 1989; Poddevin et al., 1991). However, if electroporation is to be better understood, more comprehensive, quantitative studies which determine the effects of basic parameters on molecular transport will be necessary. More specifically, quantitative determinations at the individual cell level will be needed to: 1) suggest and test theoretical models, 2) provide a basis for comparing data for different molecules and experimental conditions, and 3) guide applications of electroporation in research, biotechnology, and medicine.

Most electroporation studies have used one of the following four methods of analysis: (A) expression of an introduced gene, (B) total population methods, (C) image analysis, or (D) flow cytometry.

(A) Studies focusing on the uptake and expression of exogenous DNA by a living cell are relevant to transfection applications, but are inherently coupled to other processes. For example, whether a cell grows into a colony which expresses the introduced gene depends on many more factors than just transport of DNA across the cell membrane.

(B) Total population methods, such as turbidity changes in cell suspensions and radioactivity measurements of cell populations pulsed in the presence of radiolabeled molecules, better isolate electroporative transport, but are responsive only to the average electroporative behavior of cells. There are, however, fundamental physical and biological reasons for expecting a heterogeneous electroporation response within a cell population (Weaver and Barnett, 1992), and indeed heterogeneity is observed experimentally (Weaver et al., 1988; Liang et al., 1988; Mir et al., 1988; Lambert et al., 1990; Rosemberg and Korenstein, 1990; Tekle et al., 1991). Although the average transport per cell is of interest, it is important to determine whether the average reflects behavior of a single population with similar responses, or of two or more distinct subpopulations with significantly different responses.

(C) Image analysis of individual cells provides the power of spatial and temporal resolution. However, limitations include: 1) restricted ability to measure kinetics on the microsecond level, the time scale during which electroporation

Received for publication 17 November 1992 and in final form 31 March 1993.

Address reprint requests to Robert Langer or James C. Weaver.

0006-3495/93/07/414/09 $2.00

phenomena are believed to occur, based on experimental observations (Benz et al., 1979; Benz and Zimmermann, 1980; Hibino et al., 1991) and on theoretical grounds (Barnett and Weaver, 1991; Weaver and Barnett, 1992); 2) difficulty in observing molecules entering cells (as opposed to those exiting), even though it is uptake which is relevant to most applications (Weaver and Barnett, 1992); and 3) restriction to measuring only a few cells at a time, with the consequence that population distributions of behavior are difficult to obtain.

(D) Flow cytometry provides large numbers of quantitative optical measurements on individual cells at rates of 10^2 to 10^4 cells/s (Shapiro, 1988; Melamed et al., 1990). Although flow cytometry is not attractive for measuring rapid kinetics, it provides quantitative and statistically significant end point measurements on large numbers of individual cells. Molecular uptake and cell damage can be independently assessed. Light scatter is responsive to morphology and calibrated fluorescence provides a quantitative measurement of the number of fluorescent molecules. At their present performance levels, image analysis and flow cytometry are complementary, with neither able to provide all of the important types of measurements.

In this study we have used flow cytometry because of its quantitative nature at the single cell level, to conduct a systematic study of the effects of electric field strength (single exponential pulse) on molecular transport due to electroporation of four molecules with different physical characteristics. We have chosen erythrocyte ghosts as model cells because of the following advantages: 1) large, consistent supply from which ghosts are easily prepared, 2) relatively simple spherical geometry for most ghosts, and 3) existence of many previous electroporation studies (Sale and Hamilton, 1968; Auer et al., 1976; Zimmermann et al., 1976; Kinosita and Tsong, 1977; Chang and Reese, 1990; Dimitrov and Sowers, 1990). Because electroporation has been shown to occur universally in lipid bilayers, irrespective of the details of their composition (Neumann et al., 1989; Chang et al., 1992), results from red blood cell ghosts are expected to be representative of cells in general. However, disadvantages include: 1) heterogeneity of red blood cell ghost size, shape, and age in usual preparations (including ours) and 2) likely existence of a single, persistent defect (pore) in each ghost as the result of ghost formation (Lange et al., 1982; Lieber and Steck, 1982a; Lieber and Steck, 1982b).

EXPERIMENTAL METHODS

Red blood cell ghost preparation

Human blood is obtained from healthy adult volunteers and heparinized (Vacutaner tube; Becton Dickinson, Franklin Lake, NJ); red blood cells are separated and washed at least three times with Dulbecco's phosphate-buffered saline (PBS; pH 7.4; 149 mM total salts: 8.0 g/liter NaCl, 1.15 g/liter Na_2HPO_4, 0.2 g/liter KCl, 0.2 g/liter KH_2PO_4) (centrifugation at 450 *g*, 12 min, 4°C). Red blood cells are then immediately converted into erythrocyte ghosts by hypotonic lysis (5 mM PBS, pH 8.5, 20 min; washed four times with 20 mM PBS, pH 8.5, centrifuge at 10,000 *g*, 20 min, 4°C (Dodge et al., 1963). Ghosts are stored as a pellet at 4°C and used within 4 days.

To preload ghosts with calcein, after lysis and one wash, ghosts are placed in lysis buffer (5 mM PBS, pH 8.5) containing 10^{-3} M calcein at 4°C for 1 h. Then, an equal volume of resealing buffer (40 mM PBS, pH 8.5) containing 10^{-3} M calcein is added, and the mixture is stored at 22–24°C for 2 h. Ghosts are then washed four times and stored as above.

Electroporation protocol

About 10^7 ghosts/ml were suspended in PBS (20 mM, pH 8.2 ± 3) containing 10^{-4} M calcein (lot 10A-3; Molecular Probes, Eugene, OR) or 10^{-5} M of one of the following fluorescent macromolecules: 1) fluorescein-labeled lactalbumin (lot 9A; Molecular Probes), 2) fluorescein-labeled bovine serum albumin (BSA; lot 10C, Molecular Probes), or 3) fluorescein isothiocyanate-dextran (average molecular mass = 71 kDa, lots 105F-5029 and 118F-0821, Sigma Chemical Co., St. Louis, MO). Unlike proteins, with known molecular weight and structure, dextrans have distributions in size. One therefore does not know if uptake of dextran molecules represents transport of dextrans of all molecular weights or of, for example, only the dextrans of low molecular weight. In spite of this disadvantage, many investigators have used them (Sowers and Lieber, 1986; Weaver et al., 1988; Liang et al., 1988; Bartoletti et al., 1989; Dimitrov and Sowers, 1990; Rosemberg and Korenstein, 1990).

Pulsing is performed either at room temperature (22–24°C) or at 0–4°C with a Gene Pulser (Bio-Rad, Richmond, CA) or an Electro Cell Manipulator 600 (Biotechnologies and Experimental Research, San Diego, CA) and with 2-mm gap cuvettes with parallel-plate aluminum electrodes (Bio-Rad). Cuvettes are reused up to 10 times each. Exponentially decaying electric field pulses (exponential decay time constant, τ, between 1 and 2 ms) of various magnitudes are used. 5 min after the pulse, ghosts are washed twice with PBS (20 mM, pH 8.2 ± 3; centrifuge at 10,000 *g*, 3 min, room temperature), suspended in PBS (20 mM, pH 8.2 ± 3) containing fluorescent latex microspheres ("beads"; ~10^6/ml; d = 5.8 μm; Polysciences, Warrington, PA) and stored at 0–4°C until analysis the same day.

The nominal electric field is determined by dividing the voltage (displayed by the pulsing device) by the electrode gap: $E_{nominal} = V_{output}/d_{electrode}$. However, if significant potential drops exist outside the ghost suspension (e.g., at the electrode/electrolyte interfaces), the field to which the ghosts are exposed will be lower. In this study, we determine the actual field within the ghost suspension using a method described previously (Bliss et al., 1988): we measure the ghost suspension electrical conductivity, measure the current through the cell suspension by placing a 5-ohm resistor in series with the cuvette, and then compute the electric field pulse magnitude within the ghost suspension. We have found no significant potential drops outside the ghost suspension, which demonstrates that in this study the nominal field is the same as the actual field.

After most experiments had been performed, it was brought to our attention that pulsing with standard cuvettes can cause pH shifts. Since our system is only weakly buffered, pH changes occurred (final range between pH 8 and 9), which increased with pulse voltage. To assess the effect of pH, we performed additional studies of BSA uptake at different voltages using $7.4 \leq pH \leq 10$. In each case the uptake versus voltage graph (i.e., see Fig. 6) was of the same form (plateau observed), and the absolute values of molecular transport between pH 8 and 9 were within 20% of each other. We therefore conclude that pH has only a weak effect on uptake under the conditions of our experiments.

In summary, upon electroporation resulting in sufficiently large pores in the ghost membrane, fluorescent molecules are able to enter the ghosts. After waiting 5 min and then washing the ghosts, fluorescent molecules inside the ghosts can be measured by the flow cytometer. Fluorescent beads are co-suspended (at a fixed concentration) with the ghosts as an internal volumetric standard. This provides a basis for determining if ghosts are destroyed by electroporation or otherwise lost during sample handling and washing: determination of the ghost/bead ratio provides a relative ghost concentration which can be compared to control samples.

Flow cytometry measurements

Individual measurements on ghosts and beads are performed by a FACStar Plus flow cytometer (Becton Dickinson) using Consort 40 software (Becton

Dickinson) on a microVAX computer (Digital Equipment Corp., Maynard, MA). Fluorescence data are collected using a custom-modified three or four-log decade amplifier; collection of scatter data is with a standard four-log decade amplifier. Multiple optical measurements are made at a rate of up to 3000 ghosts/s, which allows rapid collection of large amounts of statistically meaningful data at the individual ghost level. Ghosts are diluted into a carrier fluid (Isoton II balanced electrolyte solution; Coulter Diagnostics, Hialeah, FL) and passed through a 488-nm laser beam (Innova-90 argon ion laser; 5 W; Coherent, Palo Alto, CA). Measurements of light scatter of the ghosts give an indication of object size and shape, allowing discrimination between ghosts, microspheres, and debris. With calibration, fluorescence measurements provide a quantitative determination of the number of fluorescent molecules associated with each ghost. Microscopy of electroporated ghosts generally shows uniformly fluorescent solid circles, as opposed to fluorescent rings, supporting the interpretation that ghost fluorescence is due to molecules inside the ghost rather than molecules bound to the membrane.

In a typical experiment in this study, measurement of ghost fluorescence proceeds as follows: as a ghost passes through the flow cytometer, it scatters light from the laser. This triggers collection of light scatter and fluorescence data (90° light scatter trigger used). Fluorescein is excited at 488 nm, and the resulting fluorescence emission is collected through a 530-nm band pass filter.

Quantitative fluorescence calibration

Quantitative calibration beads (Flow Cytometry Standards; Research Triangle Park, NC) are used to convert fluorescein fluorescence measurements into quantitative numbers of molecules contained inside each ghost (Bartoletti et al., 1989). These calibration beads provide the equivalent fluorescence of specified numbers of fluorescein molecules free in solution. For example, one bead may be as bright as 10^6 free fluorescein molecules. However, our fluorescent tracer molecules may fluoresce differently from free fluorescein, e.g., 10^6 lactalbumin molecules with multiple bound-fluorescein labels may have a different fluorescence intensity than 10^6 free fluoresceins. Therefore, the fluorescence of each type of fluorescent molecule must be determined relative to that of free fluorescein before proper calibration can be done. This is accomplished by comparing the fluorescence intensities of known concentrations of each fluorescent molecule to that of known concentrations of free fluorescein (lot 20H-3413; Sigma Chemical Co.) in a spectrofluorimeter (Fluorolog-2, model F112AI; Spex Industries, Edison, NJ), using the same filter for collection of fluorescent light as is used in the flow cytometer. Sample excitation is performed at 488 nm with a 4.6-nm bandwidth. Under the conditions of this study, the ratios, R, of fluorescent molecule fluorescence to free fluorescein fluorescence are: $R_{\text{calcein}} = 0.65 \pm 0.28$, $R_{\text{lactalbumin}} = 0.51 \pm 0.26$, $R_{\text{BSA}} = 1.11 \pm 0.39$, $R_{\text{dextran}} = 3.05 \pm 0.61$ (lot 105F-5029) and 1.63 ± 0.62 (lot 118F-0821). The error ranges are attributed to different degrees of fluorescent sample bleaching.

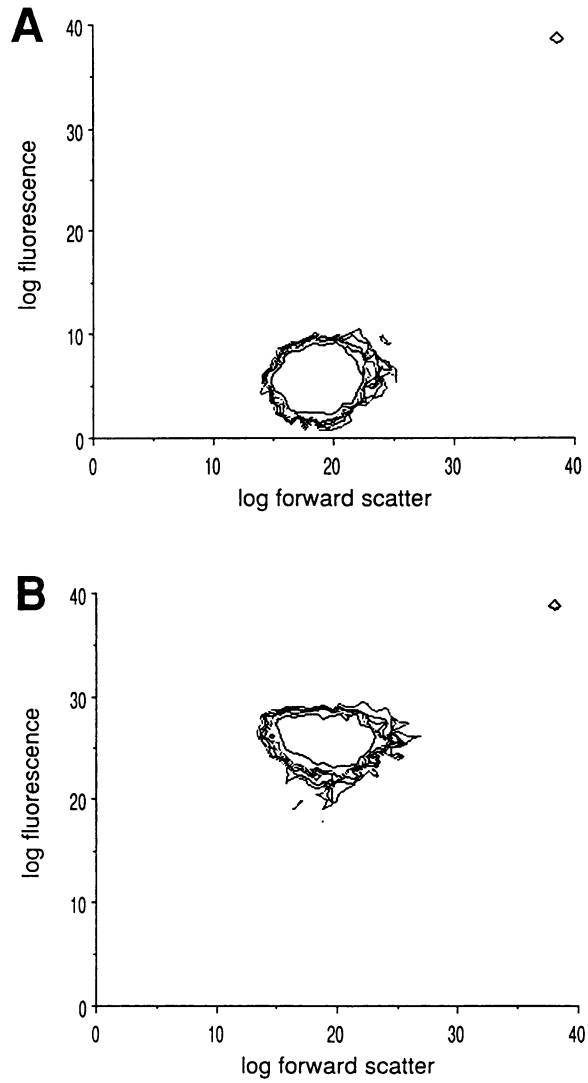

FIGURE 1 Typical log contour plots of fluorescence versus forward scatter. Obtained from flow cytometry data, *A* shows a population of control (unpulsed) ghosts with low fluorescence; this is believed to be mainly due to a combination of autofluorescence, "background" surface binding of fluorescein-labeled BSA to ghosts, and flow cytometer noise. *B* shows a population of ghosts exposed to a 6-kV/cm pulse with high fluorescence, indicating uptake of fluorescein-labeled BSA molecules. Reference beads comprise the population of events in the upper right corner; see Experimental Methods for discussion.

RESULTS

Flow cytometric measurements are displayed as two-dimensional contour plots and one-dimensional histograms for red blood cell ghost populations exposed to a single exponential electric pulse, of magnitude ranging from 0 to 8 kV/cm, and with a time constant between 1 and 2 ms. Fig. 1 is a typical log-log contour plot showing forward scatter (which is sensitive to ghost morphology) versus fluorescence (which provides a measure of the number of fluorescent molecules inside each ghost, after calibration). The lines on these contour plots represent iso-frequency-of-occurrence values for light scatter and fluorescence. Each plot represents data from approximately 20,000 ghosts.

Fig. 1 *A* shows a control (unpulsed) population of ghosts not subjected to an electric pulse. Some background fluorescence is evident (autofluorescence, BSA surface binding, flow cytometer noise). Fig. 1 *B* shows a population of ghosts with higher fluorescence, indicating uptake of BSA molecules by ghosts due to electroporation. Also, in the upper right corner is a small population of co-suspended reference beads (large forward scatter and fluorescence), which are used to measure the loss of any ghosts as a result of electroporation or the washing procedure.

The distributions of net molecular transport per ghost are presented as one-dimensional log histograms. Fig. 2 shows representative histograms of ghost fluorescence (or molecular uptake) from three individual samples pulsed at different field strengths. While fluorescence/uptake increases at

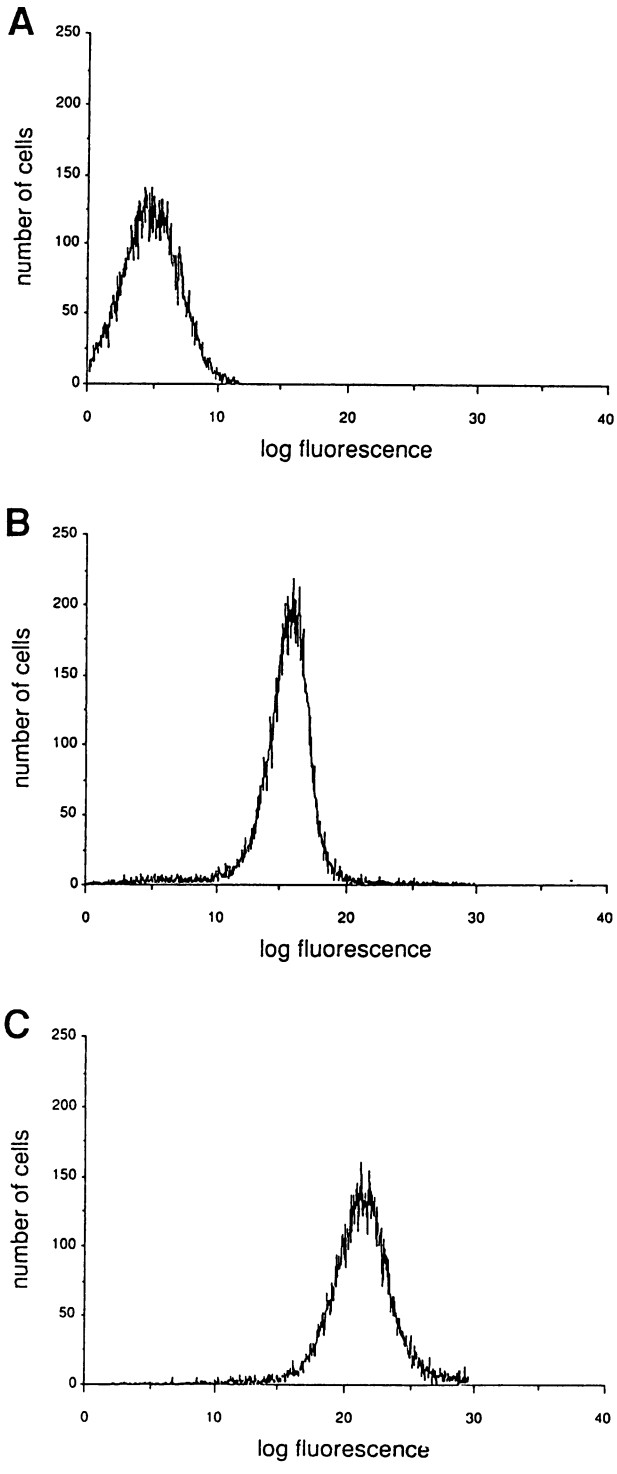

FIGURE 2 Fluorescence histograms showing uptake of fluorescein-labeled BSA by control (unpulsed) ghosts (*A*), and by ghosts exposed to a small field (2 kV/cm) (*B*) and a large field (8 kV/cm) (*C*). The vertical axis gives the number of events (ghosts only; beads and debris have been edited out), and the horizontal axis gives fluorescein fluorescence (here arbitrary units). The existence of a single population of ghosts is evident in each case, although the amount of molecular transport varies widely within each population.

higher field strengths, the existence of a single population of ghosts is evident in each case. As expected for spherical membranes with a range of sizes, all ghosts appear to respond to a given pulse in a similar way: no subpopulations exist.

These distributions, however, exhibit a large range in fluorescence for both the control and pulsed ghosts (average coefficients of variation for electroporated ghosts are approximately 100%); heterogeneity of response is evident. Moreover, more pronounced heterogeneity is seen in other samples, particularly at lower field strengths. For example, sometimes (<1%) two subpopulations are seen: one at lower fluorescence (similar to controls) and one at higher fluorescence. Broader distributions, including trailing edges at lower fluorescence, are also sometimes present. While these deviations are frequently observed, they are not consistent or reproducible; they do not support any identifiable trend. We interpret these data as meaning simply that there is heterogeneity in electroporation, both in the ghosts as well as in the experimental conditions. Sources of heterogeneity are discussed below.

Individual ghost fluorescence can be converted to an equivalent absolute number of fluorescent molecules in that ghost. Fig. 3 shows the average uptake of calcein versus field strength. The results of Fig. 3 indicate that significant calcein transport first occurs at about 0.5–1 kV/cm, increases as field strength increases, and plateaus at approximately 1.5–2 kV/cm. The plateau uptake value of approximately 6×10^4 molecules per ghost remains up to 8 kV/cm.

Fig. 4 shows a complimentary result, in which ghosts are each loaded with an average of about 8×10^5 calcein molecules before pulsing, so that release due to electroporation can be observed. As in Fig. 3, net calcein transport first occurs at approximately 1 kV/cm and achieves a maximum efflux at and above approximately 2 kV/cm. In the plateau region, where fluorescence corresponds to an average of less than 4×10^4 calcein molecules, release is at least 95% complete. The inability of progressively larger pulses to further

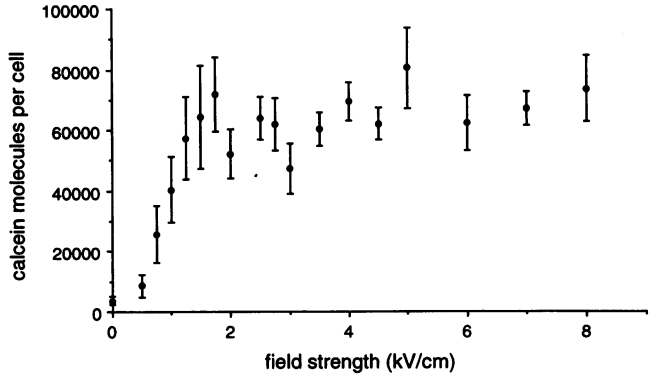

FIGURE 3 Uptake of calcein by ghosts as a function of pulse magnitude. Above approximately 0.5–1 kV/cm, uptake increases with field strength, while above approximately 1.5–2 kV/cm, a plateau is observed. Graphs in Figs. 3 through 8 each include data from on the order of 10^6 individual ghosts; each point represents the average of between four and 30 samples collected during at least three different experiments.

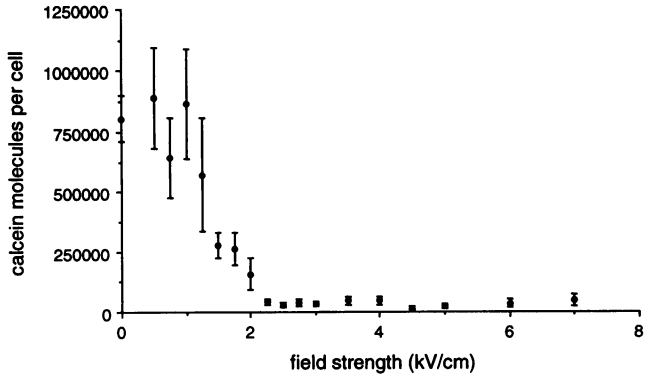

FIGURE 4 Release of calcein from preloaded ghosts as a function of pulse magnitude. Calcein transport out of ghosts increases and then plateaus at approximately the same field strengths as calcein transport into ghosts (Fig. 3).

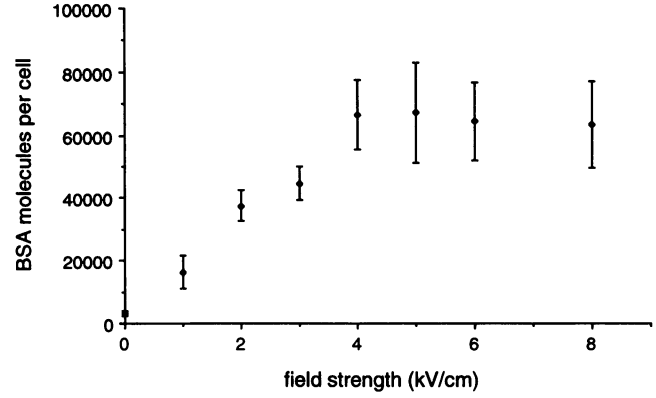

FIGURE 6 Uptake of fluorescein-labeled BSA by ghosts as a function of pulse magnitude. Above approximately 1 kV/cm, uptake increases with field strength, while above approximately 4 kV/cm a plateau is observed.

reduce average ghost fluorescence is probably due to ghost autofluorescence, calcein surface binding, and flow cytometer noise.

Similar molecular transport behavior is found for fluorescence-labeled lactalbumin, BSA, and dextran (Figs. 5, 6, and 7). In these cases, however, the extracellular concentration is 10-fold lower (10^{-4} M for calcein, 10^{-5} M otherwise). Nevertheless, for all cases, an initial region exists where uptake increases with field strength, which is followed by a plateau region where transport appears independent of field strength. However, there are significant quantitative differences (Table 1).

Finally, Fig. 8 shows the number of ghosts "lost" by the electroporation process. At field strengths greater than 1 kV/cm, approximately 30% of ghosts are "lost," determined as follows. Ghosts have known light scatter characteristics; by gating, only events which scatter like ghosts (or reference beads) are used in the analysis. A constant concentration of reference beads is present in each sample, so that the ratio of ghosts per bead is proportional to the ghost concentration. Since all samples have the same initial ghost concentration

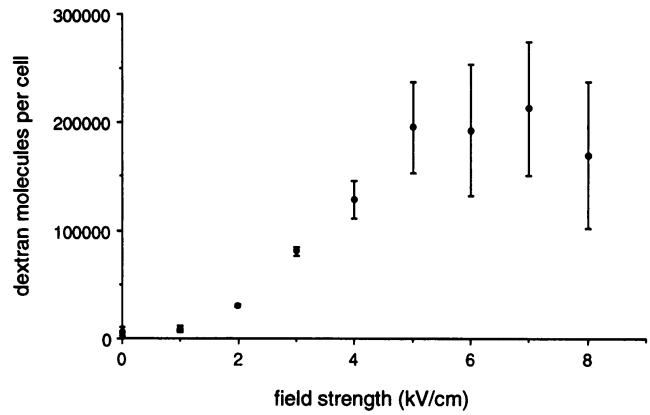

FIGURE 7 Uptake of fluorescein-labeled dextran (71 kDa average molecular mass) by ghosts as a function of pulse magnitude. Above approximately 1–2 kV/cm, uptake increases with field strength, while above approximately 5 kV/cm a plateau is observed.

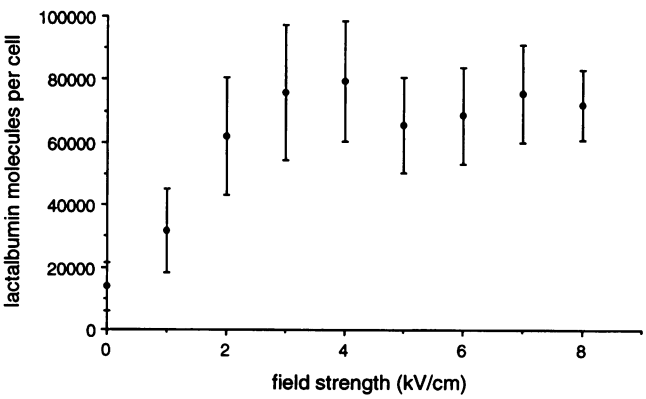

FIGURE 5 Uptake of fluorescein-labeled lactalbumin by ghosts as a function of pulse magnitude. Above approximately 1 kV/cm, uptake increases with field strength, while above approximately 2–3 kV/cm a plateau is observed.

(and therefore the same ghosts per bead ratio), it is possible to identify what percent of ghosts are "lost" during the experimental protocol. Data for Fig. 8 come from the experiments shown in Figs. 3–7 and other similar experiments where fluorescent tracer molecules have been present.

DISCUSSION

Molecular transport plateau

For the single exponential pulse used, the uptake of four very different molecules exhibits qualitatively similar behavior. There appear to be two domains of transport: a sub-plateau domain at lower field strengths and a plateau domain at higher field strengths. In the sub-plateau domain, transport increases with increasing field strength, indicating that electrically driven phenomena (e.g., electrical drift, electroosmosis, pore population characteristics) control the transport. In the plateau domain, transport occurs independent of field strength, suggesting that electrically driven phenomena may not control transport. The existence of such a plateau in

TABLE 1 Summary of the basic features of molecular transport behavior

Molecule	Transport threshold	Plateau characteristics	"Equilibrium" at plateau
	kV/cm		%
Calcein (623 Da, −4 charge)	0.5–1	1.5–2 kV/cm; 6×10^4 molec/cell	0.7
Lactalbumin (14.5 kDa, −15 charge)	<1	2–3 kV/cm; 6×10^4 molec/cell	7
BSA (68 kDa, ~−25 charge)	<1	4 kV/cm; 6×10^4 molec/cell	7
Dextran (71 kDa average, −4 charge*)	1–2	5 kV/cm; 2×10^5 molec/cell	20

Plateau concentrations have been calculated by averaging the numbers of molecules per ghost in the plateau region and then subtracting the average number of molecules per ghost in controls. Percent "equilibrium" is a measure of how close the probe concentration inside the ghosts is to the supplied external concentration.

* Associated with fluorescein label.

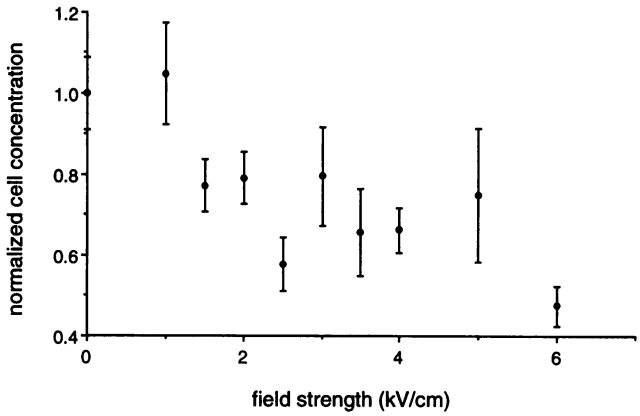

FIGURE 8 Normalized ghost concentration versus pulse magnitude showing destruction or loss of ghosts because of electroporation. Significant numbers of ghosts are destroyed at field strengths above 1 kV/cm. See Results for calculation methods and discussion.

uptake has not been reported before. This is not surprising, given that most previous studies have characterized transport as either occurring or not occurring; absolute amounts of transport have not been assessed.

We considered the possibility that artifact or error may have caused this transport plateau. However, 1) we have verified that the actual electric fields which the ghosts experience are the fields selected on the pulser. Moreover, the plateau occurs at different pulse magnitudes for different molecules, also indicating that the pulser is not malfunctioning. 2) We have observed this trend with four different molecules. 3) Upon varying the time between pulsing and washing up to 1 h, we find that the plateau still exists. This suggests that molecules are not coming back out of ghosts due to premature washing. 4) Finally, we continue to find pulse-amplitude plateaus in uptake under other conditions (e.g., multiple pulses, longer pulses, different external molecule concentrations), although the plateau transport value is different (unpublished data). For these reasons we believe that this plateau is real.

A plateau could be easily explained if the molecular concentration inside the ghost at the plateau were equal to its concentration outside the ghost, as there would be no net transport. However, plateau values of the intracellular fluorescent-molecule concentration (e.g., 6×10^4 molecules/ghost or 7×10^{-7} M) correspond to between 0.7 and 20% of the external concentration at the time of the pulse (Table 1). Since ghosts are believed to be essentially "empty" spherical membranes, with negligible cytoplasmic residue, an equilibrium altered by the content of the ghost's interior, such as a Donnan equilibrium associated with a negatively charged cytoplasm, can be excluded. Moreover, microscopy shows that in most cases ghosts appear as uniformly fluorescing solid circles, not fluorescent rings. This suggests that molecules are distributed within the interior of the ghosts and not binding to the membrane. Finally, other studies indicate that this uptake plateau can be exceeded by altering other electrical parameters (e.g., number of pulses) (unpublished data). Therefore, this plateau is not an absolute maximum in uptake by the ghosts, but rather indicates a maximum effect of increasing field strength.

Considering mechanisms by which transport occurs, Dimitrov and Sowers (1990) suggest that molecular efflux from erythrocyte ghosts is controlled by electro-osmosis. Others, however, argue that uptake of DNA by intact cells is controlled by DNA electrophoresis (Klenchin et al., 1991). In either case, transport is governed by the electric field, and increasing pulse magnitude is expected to increase transport. That a plateau in transport is observed at high field strengths suggests that molecular uptake may be a multistep process: at lower field strengths, an electric-field-dependent step, such as electro-osmosis or electrophoresis, is rate-limiting. However, when this step becomes very fast at higher field strengths, a different step, which does not depend on electric field strength, becomes rate-limiting. The exact nature of this second step is unclear, but could involve diffusion. Observations presented by Abidor and Sowers (1992) on electrofusion, an electroporation-related phenomenon, also suggest a two-step process. They find that, at lower electric field strengths, fusion rate increases strongly with increasing field magnitude, while at higher field strengths, fusion rate increases only moderately with increasing fields. Although they propose a single step mechanism, it would instead appear that at lower field strengths a single voltage-dependent step is rate-limiting and, after a sharp transition, at higher field strengths a different single weakly voltage-dependent step is rate-limiting. Other possible hypotheses for the observed plateau behavior include: 1) diffusion controls transport, 2) increased field strength does not alter pore population characteristics in ways which affect transport, 3) there is a

limited effective volume inside the ghost available to entering molecules, and/or 4) there is no net effect generated by the sum of a number of electrically governed parameters.

We have considered hypotheses which could explain our results, but concluded that this data, even when combined with other information in the literature, is insufficient to conclusively support any one mechanism by which a plateau in transport is achieved. This plateau is probably a consequence of the detailed, interactive behavior of a dynamic pore population, the transmembrane voltage, and one or more molecular transport mechanisms. Presently the microscopic mechanisms by which molecules are transported across a cell membrane due to electroporation are poorly understood; they presumably include diffusion, electrophoresis of molecules and cells, and electro-osmosis. Although some progress has been made, the ability to make complete quantitative predictions of molecular transport which are consistent with known electrical behavior of the cell membrane does not yet exist. With this in mind, the present results present a challenge to the development of models of electroporation and its associated molecular transport.

A final consideration concerns the quantitative differences in uptake between the four molecules investigated. These molecules can be ranked in order of decreasing charge density: calcein (−4 charge/623 Da = 6×10^{-3} e/Da) > lactalbumin (−15 charge/14.5 kDa = 1×10^{-3} e/Da) > BSA (~−25 charge/68 kDa = 4×10^{-4} e/Da) > dextran (−4 charge/71 kDa = 6×10^{-5} e/Da). Examination of the plateau characteristics summarized in Table 1 shows that the plateaus begin at higher field strengths for molecules with lower charge densities; the field strength at which the plateau is achieved correlates inversely with molecule charge density. This suggests that the transition from electrically controlled transport to field-independent transport occurs at a lower field strength for a molecule with a higher charge density.

The different plateau concentrations of macromolecules inside ghosts also correlate inversely with charge density (see Table 1). Calcein was present at an external concentration of 10^{-4} M. It has an internal plateau concentration $\approx 6 \times 10^4$ molecules/150 μm^3 (erythrocyte ghost volume (Sowers and Lieber, 1986)) $\approx 7 \times 10^{-7}$ M, or approximately 0.7% of the external concentration. Lactalbumin and BSA, at external concentrations of 10^{-5} M, have internal plateaus at 7% of the external concentration. Finally, dextran, at 10^{-5} M externally, plateaus at 20% of the external concentration. There appears to be a trend of increasing relative plateau concentration with decreasing charge density.

Even though present externally at different concentrations, the absolute number of molecules inside each cell is approximately the same for calcein and lactalbumin or BSA. This appears to be coincidental. Other studies indicate that internal plateau concentration is a function of external concentration and indicate that, had calcein been present at 10^{-5} M, its uptake would have been significantly lower (unpublished data). Also, different transport plateau values have been found under a variety of different conditions (unpublished data). This argues against some sort of receptor binding limiting the plateau concentration to the order of 100,000 molecules/cell. Moreover, repeated examination under the microscope shows fluorescence throughout electroporated cells, indicating that uptake is not localized, for example, within the membrane.

Population distributions

Fluorescence histograms, such as Fig. 2, show that no significant subpopulations of ghosts exist; all ghosts respond to a given electric-field pulse in a similar manner. This is not surprising for spherically symmetric ghosts, since many of the possible sources of variation in response are related to the relative size and orientation of asymmetric cells (Weaver and Barnett, 1992). Exceptions, however, are sometimes observed where two subpopulations coexist and/or where population distributions become much broader. These are especially evident at field strengths where transport due to electroporation begins (e.g., 1 or 2 kV/cm). Sources of this heterogeneous behavior might include: 1) ghosts which are not spherical and/or are not the same size (both are supported by microscopy), and 2) possibly variable membrane properties due to ghost age (inherent to erythrocytes) and interghost variability.

Despite these inhomogeneities, in most cases only one population of ghosts is found, consistent with the widely held view that electroporation occurs universally in lipid bilayer membranes if the transmembrane potential is raised to of order 1 V; approximately 0.5–1 V for short pulses (~10 μs) and 0.2–0.5 V for longer pulses (>100 μs) (Neumann, 1989). The maximum change in transmembrane voltage, $\Delta U(t)$, across a spherical cell in an imposed uniform electric field, $E(t)$, is well known at small field strengths to be (Foster and Schwann, 1986)

$$\Delta U(t) = 1.5\, E(t)\, R_{cell} \qquad (1)$$

where R_{cell} is the cell radius. In this study, molecular transport seems to first occur at less than 1 kV/cm. Using the above equation (R_{ghost} = 3.3 μm (Sowers and Lieber, 1986)), a 1-kV/cm electric field corresponds to a transmembrane voltage of approximately 0.5 V, in good agreement with the "universal" breakdown voltage of 0.2–0.5 V for longer pulses.

Direction of transport

Figs. 3 and 4 show transport of calcein into and out of ghosts. The finding that transport begins and plateaus at approximately the same field strengths indicates that the direction (influx/efflux) of transport across the membrane is not important in this case.

Destruction of ghosts

The results in Fig. 8 imply that approximately 30% of the ghosts can be destroyed by electroporation. However, these ghosts have experienced more than just exposure to an

electric-field pulse which may contribute to their destruction. First, as erythrocyte ghosts, they have been opened by osmotic swelling, have released their hemoglobin, and have then been allowed to reseal. Although this is a well established procedure (Dodge et al., 1963; Sowers and Lieber, 1986), it is not a fully reversible process, leaving the membrane permanently altered (Lange et al., 1982; Lieber and Steck, 1982a; Lieber and Steck, 1982b). Moreover, after electroporation, ghosts are washed, involving centrifugation twice at 10,000 *g*, which subjects the ghosts to mechanical stress. Nevertheless, the control preparations are subjected to these same procedures, which indicates that the exposure to the electric field pulse is responsible. From this study we conclude that significant losses of ghosts were observed at field strengths where electroporation occurs; further investigation is needed to establish whether these results showing ghost destruction can be generalized to other systems.

CONCLUSIONS

A quantitative study of molecular uptake due to electroporation is presented, including data on the transport of four different molecules from measurements of more than 10^6 individual ghosts. Under the conditions of this study, the findings are: (*a*) A single population of ghosts generally exists, indicating that all ghosts respond to a given electric field pulse in a similar manner. However, the amount of transport per ghost within this population varies widely, indicated by average coefficients of variation of approximately 100%. The onset of transport due to electroporation occurs at less than 1 kV/cm, corresponding to a transmembrane voltage of approximately 0.5 V. (*b*) After the onset of electroporation, average uptake increases with increasing field strength and then plateaus at higher field strengths. Although a detailed mechanism is not proposed, it appears that transport is controlled by electric field-dependent processes at lower field strengths, but may be controlled by electric field-independent processes at higher field strengths. Both the field strength at which the plateau is achieved and the relative internal plateau concentration appear to correlate inversely with the molecule's charge density. (*c*) The direction of transport (influx/efflux) does not appear to affect net molecular transport significantly. This result is based only on calcein transport data. (*d*) Approximately 30% of ghosts can be destroyed by the electroporation procedure. However, it is unclear whether these results can be generalized to intact cells.

We thank G. I. Harrison, G. A. Paradis, R. M. Silvera, J. H. Kim, and J. A. Levinson for general assistance in the laboratory; V. G. Bose for helping with electric field measurement validation; and S. Cohen, A. E. Sowers, W. M. Deen, A. J. Grodzinsky, and R. C. Lee for helpful discussions.

This work has been supported partially by a fellowship provided by Cygnus Therapeutic Systems (to M. R. Prausnitz), by National Institutes of Health (NIH) grant GM44884 (to R. Langer), and by Army Research Office grant DAAL03-90-G-0218 and NIH grant GM34077 (to J. C. Weaver).

REFERENCES

Abidor, I. G., and A. E. Sowers. 1992. Kinetics and mechanism of cell membrane electrofusion. *Biophys. J.* 61:1557–1569.

Auer, D., G. Brandner, and W. Bodemer. 1976. Dielectric breakdown of the red blood cell membrane and uptake of SV 40 DNA and mammalian cell RNA. *Naturwiss.* 63:391.

Barnett, A., and J. C. Weaver. 1991. A unified, quantitative theory of reversible electrical breakdown and rupture. *Bioelectrochem. Bioenerg.* 25: 163–182.

Bartoletti, D. C., G. I. Harrison, and J. C. Weaver. 1989. The number of molecules taken up by electroporated cells: quantitative determination. *FEBS Lett.* 256:4–10.

Benz, R., and U. Zimmermann. 1980. Relaxation studies on cell membranes and lipid bilayers in the high electric field range. *Bioelectrochem. Bioenerg.* 7:723–739.

Benz, R. F., F. Beckers, and U. Zimmermann. 1979. Reversible electrical breakdown of lipid bilayer membranes: a charge-pulse relaxation study. *J. Membr. Biol.* 48:181–204.

Bliss, J. G., G. I. Harrison, J. R. Mourant, K. T. Powell, and J. C. Weaver. 1988. Electroporation: the population distribution of macromolecular uptake and shape changes in red blood cells following a single 50 μs square wave pulse. *Bioelectrochem. Bioenerg.* 20:57–71.

Chakrabarti, R., D. E. Wylie, and S. M. Schuster. 1989. Transfer of monoclonal antibodies into mammalian cells by electroporation. *J. Biol. Chem.* 264:15494–15500.

Chang, D. C., and T. S. Reese. 1990. Changes in membrane structure induced by electroporation as revealed by rapid-freezing electron microscopy. *Biophys. J.* 58:1–12.

Chang, D. C., B. M. Chassy, J. A. Saunders, and A. E. Sowers, editors. 1992. Guide to Electroporation and Electrofusion. Academic Press, New York. 581 pp.

Dimitrov, D. S., and A. E. Sowers. 1990. Membrane electroporation—fast molecular exchange by electroosmosis. *Biochim. Biophys. Acta.* 1022: 381–392.

Dodge, J. T., C. Mitchell, and D. J. Hanahan. 1963. The preparation and chemical characteristics of hemoglobin-free ghosts of human erythrocytes. *Arch. Biochem. Biophys.* 100:119–130.

Foster, K. R., and H. P. Schwann. 1986. Dielectric properties of tissues. *In* CRC Handbook of Biological Effects of Electromagnetic Fields. C. Polk and E. Postow, editors. CRC Press, Boca Raton. 27–96.

Hibino, M., M. Shigemori, H. Itoh, K. Nagayama, and K. Kinosita Jr. 1991. Membrane conductance of an electroporated cell analyzed by submicrosecond imaging of transmembrane potential. *Biophys. J.* 59:209–220.

Kinosita, K., Jr., and T. Y. Tsong. 1977. Formation and resealing of pores of controlled sizes in human erythrocyte membrane. *Nature (Lond.).* 268: 438–441.

Klenchin, V. A., S. I. Sukharev, S. M. Serov, L. V. Chernomordik, and Y. A. Chizmadzhev. 1991. Electrically induced DNA uptake by cells is a fast process involving DNA electrophoresis. *Biophys. J.* 60:804–811.

Lambert, H., R. Pankov, J. Gauthier, and R. Hancock. 1990. Electroporation-mediated uptake of proteins into mammalian cells. *Biochem. Cell Biol.* 68:729–734.

Lange, Y., A. Gough, and T. L. Steck. 1982. Role of the bilayer in the shape of the isolated erythrocyte membrane. *J. Membr. Biol.* 69:113–123.

Liang, H., W. J. Purucker, D. A. Stenger, R. T. Kubiniec, and S. W. Hui. 1988. Uptake of fluorescence-labeled dextrans by 10T 1/2 fibroblasts following permeation by rectangular and exponential-decay electric field pulses. *Biotechniques.* 6:550–558.

Lieber, M. R., and T. L. Steck. 1982a. A description of the holes in human erythrocyte membrane ghosts. *J. Biol. Chem.* 257:11651–11659.

Lieber, M. R., and T. L. Steck. 1982b. Dynamics of the holes in human erythrocyte membrane ghosts. *J. Biol. Chem.* 257:11660–11666.

Melamed, M. R., T. Lindmo, and M. L. Mendelsohn. 1990. Flow cytometry and sorting. Wiley-Liss, New York. 824 pp.

Mir, L. M., H. Banoun, and C. Paoletti. 1988. Introduction of definite amounts of nonpermeant molecules into living cells after electropermeabilization: direct access to the cytosol. *Exp. Cell Res.* 175:15–25.

Neumann, E. 1989. The relaxation hysteresis of membrane electroporation. *In* Electroporation and Electrofusion in Cell Biology. E. Neumann, A. E. Sowers, and C. A. Jordan, editors. Plenum Press, New York. 61–82.

Neumann, E., A. E. Sowers, and C. A. Jordan, editors. 1989. Electroporation and Electrofusion in Cell Biology. Plenum Press, New York. 436 pp.

Poddevin, B., S. Orlowski, J. Belehradek, Jr., and L. M. Mir. 1991. Very high cytotoxicity of bleomycin introduced into the cytosol of cells in culture.

Biochem. Pharmacol. 42(suppl.):S67-S75.

Rosemberg, Y., and R. Korenstein. 1990. Electroporation of the photosynthetic membrane: a study by intrinsic and external optical probes. *Biophys. J.* 58:823–832.

Sale, A. J. H., and W. A. Hamilton. 1968. Effects of high electric fields on microorganisms: III. Lysis of erythrocytes and protoplasts. *Biochim. Biophys. Acta.* 163:37–43.

Shapiro, H. M. 1988. Practical Flow Cytometry. Alan R. Liss, New York. 295 pp.

Sowers, A. E., and M. R. Lieber. 1986. Electropore diameters, lifetimes, numbers, and locations in individual erythrocyte ghosts. *FEBS Lett.* 205: 179–184.

Tekle, E., R. D. Astumian, and P. B. Chock. 1991. Electroporation by using bipolar oscillating electric field: an improved method for DNA transfection of NIH 3T3 cells. *Proc. Natl. Acad. Sci. USA.* 88:4230–4234.

Weaver, J. C., and A. Barnett. 1992. Progress towards a theoretical model for electroporation mechanism: membrane electrical behavior and molecular transport. *In* Guide to Electroporation and Electrofusion. D. C. Chang, B. M. Chassy, J. A. Saunders, and A. E. Sowers, editors. Academic Press, New York. 91–118.

Weaver, J. C., G. I. Harrison, J. G. Bliss, J. R. Mourant, and K. T. Powell. 1988. Electroporation: high frequency of occurrence of a transient high-permeability state in erythrocytes and intact yeast. *FEBS Lett.* 229:30–34.

Zimmermann, U., F. Riekmann, and G. Pilwat. 1976. Enzyme loading of electrically homogeneous human red blood cell ghosts prepared by dielectric breakdown. *Biochim. Biophys. Acta.* 436:460–474.

Correction

Dr. A. La Monaca should not have been listed as an author of "X-ray small angle scattering of the human transferrin protein aggregates. A fractal study" which was published in *Biophys. J.* 64:520–524 (1993).